A Theory of Stationary Long Waves. Part II: Resonant Rossby Waves in the Presence of Realistic Vertical Shears

K. K. TUNG AND R. S. LINDZEN

Center for Earth and Planetary Physics, Harvard University, Cambridge, MA 02138

(Manuscript received 30 July 1978, in final form 24 February 1979)

ABSTRACT

In Part I a simple theory of resonant Rossby waves in a uniform zonal flow was developed. The present paper extends the previous results to the case of an atmosphere with winds varying with height. The wave responses to a large number of physically possible wind configurations are studied to help determine whether the observed wind fields in the winter atmosphere permit resonance of the large-scale waves and, in cases where resonance is possible, to search for the most favorable conditions for resonance. It is found that an increase in stratospheric jet strength and the descent of the stratospheric jet are both capable of exciting the resonant waves of zonal wavenumbers 1 and 2, with the latter (the descent of the stratospheric jet) being most effective in resonating the large-scale waves. The shorter waves (with zonal wavenumbers 3, 4 and up) are found to be insensitive to changes in wind conditions in the stratosphere as they are mostly trapped in the troposphere. These waves are easier to excite by changes in the wind conditions in the lower atmosphere. This finding may account for the higher frequency of occurrence of tropospheric blocking phenomena caused by the shorter waves (wavenumbers 3, 4 and up). The occurrence of large-scale (wavenumbers 1 and 2) blockings is seen to be relatively rare and is found to be usually accompanied by changes in stratospheric wind conditions.

1. Introduction

A conspicuous feature of the mean zonal flow in the wintertime atmosphere is that the westerlies generally increase in magnitude with height. The mean zonal wind speed in the lower troposphere is usually quite low, about 10 m s^{-1} or less, even in a sudden warming year when abnormally high winds are recorded in the upper stratosphere. It is clear that in such an atmosphere the planetary waves cannot be evanescent throughout the whole depth of the atmosphere as in the uniform wind model presented in Part I.

The long waves are vertically propagating in the lower troposphere. What happens to these waves in the upper atmosphere is of crucial importance insofar as resonance is concerned. It will be shown that resonance (or near resonance) tends to be difficult to achieve for waves that propagate freely to the top of the atmosphere. Only internally trapped waves (i.e., waves that are evanescent above some height) are capable of resonance, though near resonance can sometimes be possible for waves that do not have a real turning point but, nevertheless, have a major portion of their energy reflected back to the surface. The wave with zonal wavenumber 4 can be shown to be internally trapped, usually below the tropospheric jet maximum. This wave is capable of being resonantly excited, and may be the cause of the frequent blocking activities observed in the lower troposphere.[1] The longer waves, with wavenumbers 1 and 2, on the other hand, are nonevanescent up to at least the stratospheric jet maximum, which is usually located at ~60–70 km. Little reflection of the waves occurs below the jet maximum, due to the fact that the positive shear at the jet base tends to enhance vertical propagation. Given the fact that the damping due to radiative effects is quite large at these heights, the waves will probably be dissipated appreciably before being reflected from above the 60–70 km level. Also, the waves are more susceptible to dissipation along the wave path if the wave path is long.

Preceding the onset of major stratospheric sudden warmings (which is always accompanied by large-scale tropospheric blocking), it is generally observed that winds increase in speed at the rocketsonde levels. We attempt to determine whether the observed increase in wind speed would lead to increased trapping of the long waves (with wave-

[1] Waves with still higher wavenumbers are even more readily excited. However, the blockings caused by these waves would presumably have shorter scales, smaller amplitudes and shorter damping time scales.

0027-0644/79/060735-16$08.00

numbers 1 and 2), thus lowering the height of the turning point where the waves become evanescent and shortening the wave paths. Unfortunately, the sparse observation data available do not permit a definite conclusion to be drawn, since the location of the turning point is determined not only by the speed of the wind, but also by its shear and curvature. The approach taken here is to *construct* a range of possible wind profiles consistent with observations and determine, within reasonable limits, which if any of the wind configurations would lead to resonance. Based on such a study, we predict that, in order to have wavenumber 1 and 2 resonant, a stratospheric jet maximum probably has to descend to, or a second maximum must be created at, approximately the 40 km level so that the waves are evanescent above the middle stratosphere. Such a descent of the jet is consistent with the observational evidence available below the 30 km level. It should be pointed out, however, that the observational evidence at these levels is also consistent with a wind configuration that does not involve the descent of the jet maximum but a general increase in wind speeds at all levels above the middle stratosphere, i.e., a stratospheric jet located at the usual position of 60–70 km with an increased jet strength. It seems that resonance is unlikely in such a wind configuration, if it is assumed that damping in the upper atmosphere is strong.

The governing equation and boundary condition for inviscid waves in vertical shear are discussed in Section 2. In Section 3 we point out that a wave which is mainly radiating cannot be resonated. In Section 4, the initial time behavior of a resonant wave that is internally trapped is derived. As the resonant wave amplifies to a larger amplitude, the inviscid (or linear) model ceases to be valid. Damping due to Ekman pumping is introduced in Section 5. An expression is given for the maximum amplitude achieved by a resonant wave when Ekman pumping and topographic forcing reach an equilibrium. It is found that for this equilibrium case, both the resonance condition and the vertical structure (but not the amplitude) of the resonant solution are the same as those for a steady-state inviscid forced solution. The latter is calculated by a simple one-dimensional, time-independent numerical scheme in Section 6, which then gives both the resonance condition and the vertical structure of the resonant wave. The absolute amplitude is then known using results from Section 5. In Section 7 we discuss the resonance condition and its relation to the zonal wind profile. Section 8 gives an estimate of the residence time of the wave in its vertical traverse through the atmosphere. Based on this information, the susceptibility of the wave to dissipations—especially due to photochemical dampings in the upper atmosphere—is assessed. Section 9 is a summary of the results.

2. Governing equations and formal solutions

The potential vorticity equation in the presence of vertical shear is[2]

$$\left\{\left(\frac{\partial}{\partial t}+\bar{u}(z^*)\frac{\partial}{\partial x}\right)\left[\left(\frac{\partial^2}{\partial x^2}+\frac{\partial^2}{\partial y^2}\right)+\frac{f_0^2}{S}\left(\frac{\partial^2}{\partial z^{*2}}-\frac{\partial}{\partial z^*}\right)\right]+\hat{\beta}(z^*)\frac{\partial}{\partial x}\right\}\Phi'=0, \quad (1)$$

where

$$\hat{\beta}(z^*)=\beta-\frac{f_0^2}{S}(\bar{u}_{z^*z^*}-\bar{u}_{z^*}). \quad (2)$$

The lower boundary condition at $z^*=0$ is

$$\left(\frac{\partial}{\partial t}+\bar{u}(0)\frac{\partial}{\partial x}\right)\Phi'_{z^*}\frac{H}{S}-\frac{1}{g}\frac{\partial}{\partial t}\Phi'-\frac{H}{S}\bar{u}_{z^*}(0)\frac{\partial}{\partial x}\Phi'=-w_0, \quad (3)$$

where

$$w_0=ik\bar{u}(0)h_0[e^{ikx}\sin l(y_p-y)]$$

$$l=(\tfrac{1}{2}+n)\pi/y_p, \quad n=0,1,2,\ldots \text{ (see Part I)}$$

and h_0 is the amplitude of a Fourier component of the topographic forcing. The solution to the above system consists of a stationary wave forced by w_0, plus a traveling free wave with a phase speed c, satisfying the homogeneous part of Eq. (3) at $z^*=0$. The solution can thus be assumed to be of the form[3]

$$\Phi'(x,y,z^*,t)=[e^{ikx}\sin l(y_p-y)]\times e^{z^*/2}[\phi^{(0)}(z^*)+\phi^{(1)}(z^*)e^{-ikct}]. \quad (4)$$

The forced part, $\phi^{(0)}(z^*)$, satisfies the equation

$$\frac{d^2}{dz^{*2}}\phi^{(0)}+\lambda^{(0)2}(z^*)\phi^{(0)}=0, \quad (5)$$

where

$$\lambda^{(0)2}(z^*)\equiv\frac{S}{f_0^2}\left[\frac{\hat{\beta}(z^*)}{\bar{u}(z^*)}-(k^2+l^2)\right]-\frac{1}{4}, \quad (6)$$

and the lower boundary condition

$$\phi^{(0)}_{z^*}+\left(\frac{1}{2}-\frac{\bar{u}_{z^*}(0)}{\bar{u}(0)}\right)\phi^{(0)}=-\frac{Sh_0}{H}$$

at

$$z^*=0. \quad (7)$$

The free wave obeys the following equation and boundary conditions:

$$\frac{d^2}{dz^{*2}}\phi^{(1)}+\lambda^{(1)2}(z^*)\phi^{(1)}=0, \quad (8)$$

[2] The notations are the same as those used in Part I. A list of symbols is also included as Appendix A of the present paper.

[3] The existence of quasi-normal modes in the meridional direction in the presence of zero-wind line will be discussed in Part III. Also see Part I for a brief discussion.

$$\lambda^{(1)^2}(z^*) \equiv \frac{S}{f_0^2}\left[\frac{\hat{\beta}(z^*)}{\bar{u}(z^*) - c} - (k^2 + l^2)\right] - \frac{1}{4}, \quad (9)$$

and

$$\phi^{(1)}_{z^*z^*} + \left[\frac{1}{2} - \frac{\bar{u}_{z^*}(0)}{\bar{u}(0) - c} + \frac{c}{\bar{u}(0) - c}\frac{S}{gH}\right]\phi^{(1)} = 0$$

at

$$z^* = 0. \quad (10)$$

We are interested mainly in two types of forced solutions: radiating and internally trapped waves. The radiating wave is the relevant solution when

$$\lambda^{(0)^2}(z^*) > 0, \quad z^* \geq 0,$$

while the internal wave solution holds when there exists a turning point z_T^* in the domain, i.e.,

$$\lambda^{(0)^2}(z^*) > 0, \quad z^* < z_T^*,$$
$$\lambda^{(0)^2}(z^*) < 0, \quad z^* > z_T^*.$$

For the first case, the radiating solution can be written in the phase integral form (see Appendix B)

$$\phi^{(0)}(z^*) = A \exp\left[i\int_0^{z^*} \alpha^{(0)}(z^*)dz^*\right], \quad \mathrm{Re}\alpha^{(0)} > 0, \quad (11)$$

where $\alpha^{(0)}(z^*)$ satisfies

$$\alpha^{(0)^2} - i\frac{d}{dz^*}\alpha^{(0)} = \lambda^{(0)^2}(z^*). \quad (12)$$

For the second case, for $z^* \leq z_T^*$, the internal wave solution can be written as (see Appendix B)[4]

$$\phi^{(0)}(z^*) = \frac{A}{[\alpha_r^{(0)}(z^*)]^{1/2}} \times \sin\left[\int_{z^*}^{z_T^*} \alpha_r^{(0)}(z^*)dz^* + \frac{\pi}{4}\right], \quad (13)$$

where $\alpha_r^{(0)}$ is the real part of $\alpha^{(0)}$ satisfying (12). Above the turning point, the solution is

$$\phi^{(0)}(z^*) = \tfrac{1}{2}Ae^{-i\pi/4} \exp\left[-\int_{z_T^*}^{z^*} \gamma^{(0)}(z^*)dz^*\right], \quad (14)$$

where

$$\left.\begin{aligned} &\mathrm{Re}\gamma^{(0)}(z^*) \geq 0, \quad z^* \geq z_T^* \\ &\gamma^{(0)^2} - \frac{d}{dz^*}\gamma^{(0)} = -\lambda^{(0)^2}(z^*) \end{aligned}\right\}. \quad (15)$$

[4] The form of the solution in (13) is similar to the WKB solution and indeed it would become so if $\alpha^{(0)}(z^*)$ is replaced by $\lambda(z^*)$ in a WKB approximation. However, while the WKB is not valid near the turning point z_T^* and has to be matched to the Airy type solution there, the solution in (13) is uniformly valid for $z^* \leq z_T^*$.

In the next two sections, the radiating and internally trapped wave solutions will be examined separately.

3. The radiating wave solution

The radiating wave has a positive (upward) energy flux. Physically it is clear that no resonant buildup of the wave is possible in such a system. This fact can also be shown mathematically without difficulty.

The forced stationary wave becomes resonant when the solution is such that it satisfies the homogeneous part of the lower boundary condition (7), i.e.,

$$\phi^{(0)}_{z^*} + \left[\frac{1}{2} - \frac{\bar{u}_{z^*}(0)}{\bar{u}(0)}\right]\phi^{(0)} = 0 \quad \text{at} \quad z^* = 0.$$

When this happens, the wave can exist in the absence of forcing and would give infinite response in the presence of finite forcings, corresponding to the solution at $t = \infty$.

It can be easily shown that the radiating solution is unable to satisfy the resonance condition: Substituting the solution as given by (11) into the right-hand side of Eq. (7), one has

$$\phi^{(0)}_{z^*} + \left(\frac{1}{2} - \frac{\bar{u}_{z^*}}{\bar{u}}\right)\phi^{(0)} = \left[i\alpha^{(0)} + \frac{1}{2} - \frac{\bar{u}_{z^*}}{\bar{u}}\right]\phi^{(0)},$$

which for nontrivial solutions can never be made to vanish. Therefore, to satisfy the resonance condition, the wave has to be either internally trapped or evanescent near the lower boundary.

4. Internally trapped wave solution at resonance

Substituting the internal wave solution (13) into the lower boundary condition (7), one obtains

$$\frac{A}{[\alpha_r^{(0)}(0)]^{1/2}}\left\{-\alpha_r^{(0)}(0)\cos\left[\int_0^{z_T^*} \alpha_r^{(0)}dz^* + \frac{\pi}{4}\right] + \left[\left(\frac{1}{2} - \frac{\bar{u}_{z^*}(0)}{\bar{u}(0)}\right) - \frac{\frac{1}{2}\frac{d}{dz^*}\alpha_r^{(0)}(0)}{\alpha_r^{(0)}(0)}\right] \times \sin\left[\int_0^{z_T^*} \alpha_r^{(0)}dz^* + \frac{\pi}{4}\right]\right\} = -\frac{S\hbar_0}{H}.$$

Thus the amplitude A is found to be

$$A = -\frac{S\hbar_0[\alpha_r^{(0)}(0)]^{1/2}}{H \sin p^{(0)}(0)}\left\{-\alpha_r^{(0)}(0)\cot p^{(0)}(0) + \left[\left(\frac{1}{2} - \frac{\bar{u}_{z^*}(0)}{\bar{u}(0)}\right) - \frac{1}{2}\frac{d}{dz^*}\alpha_r^{(0)}(0)/\alpha_r^{(0)}(0)\right]\right\}^{-1}, \quad (16)$$

where

$$p^{(0)}(z^*) \equiv \int_{z^*}^{z_T^*} \alpha_r^{(0)}dz^* + \frac{\pi}{4}.$$

It is seen from (16) that resonance occurs when

$$\chi \equiv -\alpha_r^{(0)}(0)\cot p^{(0)}(0) + \left[\left(\frac{1}{2} - \frac{\bar{u}_{z^*}(0)}{\bar{u}(0)}\right) - \frac{1}{2}\frac{d}{dz^*}\alpha_r^{(0)}(0)/\alpha_r^{(0)}(0)\right] = 0, \quad (17)$$

so that

$$A = -\frac{S\hbar_0[\alpha_r^{(0)}(0)]^{1/2}}{H \sin p^{(0)}(0)}\chi^{-1} \to \infty.$$

The total solution (4) is

$$\Phi'(x,y,z^*,t) = [e^{ikx}\sin l(y_p - y)]e^{z^*/2} \times A\{\sin p^{(0)}(z^*)[\alpha_r^{(0)}(z^*)]^{-1/2} - \sin p^{(1)}(z^*)[\alpha_r^{(1)}(z^*)]^{-1/2}e^{-ikct}\}, \quad (18)$$

where

$$p^{(1)}(z^*) \equiv \int_{z^*}^{z_T^*} \alpha_r^{(1)}dz^* + \pi/4.$$

Here $\alpha^{(1)}(z^*)$ satisfies the same equation [(12)] as $\alpha^{(0)}$ except with $\lambda^{(0)^2}$ replaced by $\lambda^{(1)^2}$. To (18) one may always add a "background" free wave with an arbitrary amplitude, but it can be shown that this free wave is of little significance in terms of its influence on the mean flow.

In order for (18) to remain finite as $\chi \to 0$ at resonance, one must have $c \to 0$. Thus the condition for resonance is also the condition for the stationarity of the traveling waves. The resonant solution is to be found by taking the limits $c \to 0$ and $\chi \to 0$ using L'Hospital's rule. The details of the calculation is given in Appendix C. The result is

$$\Phi'(x,y,z^*,t) = [e^{ikx}\sin l(y_p - y)]\frac{S\hbar_0[\alpha_r^{(0)}(0)]^{1/2}}{H \sin p^{(0)}(0)\cdot F} \times \left\{\left[ikt - \cot p^{(0)}(z^*)\int_{z^*}^{z_T^*} q_r(z^*)dz^* + \tfrac{1}{2}q_r(z^*)/\alpha_r^{(0)}(z^*)\right]e^{z^*/2}[\alpha_r^{(0)}(z^*)]^{-1/2}\sin p^{(0)}(z^*)\right\}, \quad (19)$$

where F is given by (B13) and q_r is the real part of $q(z^*)$ given by Eq. (B7).

We have thus obtained the general *form* of the solution at resonance without actually going into the details of solving for functions such as $\alpha_r^{(0)}(z^*)$ and $q_r(z^*)$. The following important features of the resonant solution can be discerned from this solution:

(i) *As long as the wave is evanescent at the top portion of the atmosphere*, both the resonance condition and the solution below the turning point do *not* depend on the conditions of the atmosphere above the turning point. This result is important because it shows that the abnormal changes of the upper atmosphere that are often observed preceding the sudden warming events can have only the effect of determining the location of the turning point z_T^* and should not affect the resonance condition for internally trapped waves [see Eq. (17)]. However, since the vertical trapping of the waves is a *prerequisite* for resonance, and since the long waves with wavenumbers 1 and 2 are normally non-evanescent, the observed upper level wind changes before the warming events do seem to be important in enabling the long waves to become resonant.

(ii) Though the resonance condition $\chi = 0$ is obtained from the lower boundary condition, it is a function of the mean zonal wind over the whole region between the ground and the turning point. The resonance condition is a *nonlocal* condition.

(iii) There may, in principle, be an infinite number of wind configurations that can satisfy the single resonance condition $\chi = 0$. It will be shown that the condition is easily satisfiable with realistic wind profiles. However, some of the resonant configurations will have to be discarded as being unfavorable when damping is present.

(iv) Comparing the resonant solution (18) with that for the uniform wind case described in Part I, one sees the following similarities and differences: The time behaviors of both the sheared and non-sheared wind solutions are the same. Both grow linearly in time. The uniform wind solution also increases linearly in height in addition to the linear temporal growth. In the sheared case, the linear height variation is modified into a slightly more complicated dependence

$$\cot p^{(0)}(z)\int_{z^*}^{z_T^*} q_r(z^*)dz^* - \tfrac{1}{2}q_r(z^*)/\alpha_r^{(0)}(z^*).$$

What is more important is the fact that unlike the barotropic solution of the uniform wind case, the present resonant internally trapped wave solution has an overall amplitude that increases with height as $e^{z^*/2}$. The resonant solution in the present model can become increasingly more important at higher levels; the induced zonal wind deceleration,[5] which increases with height as $\sim e^{z^*}$, would now have the

amplitude large enough to bring down the easterly wind in the upper stratosphere.

(v) If the mean zonal wind does not vary too rapidly with height a WKB approximation can be used to give a very simple form for the resonant condition: Eq. (17). Approximating $\alpha_r^{(0)}$ by $\lambda^{(0)}$, the WKB form of χ is

$$\chi = -\lambda^{(0)}(0)\cot\left[\int_0^{z_T^*}\lambda^{(0)}(z^*)dz^* + \pi/4\right] + [\tfrac{1}{2} - \bar{u}_{z^*}^{(0)}/\bar{u}(0)].$$

Since $\lambda^{(0)}(0)$ is usually much greater than 1, the resonance condition is seen to be satisfied when

$$\cot\left[\int_0^{z_T}\lambda^{(0)}(z^*)dz^* + \pi/4\right]$$

is small, or

$$\int_0^{z_T^*}\lambda^{(0)}(z^*)dz^* = \pi/4 + j\pi, \quad j = 0, 1, 2, 3.$$

That is, in order to be resonant, the internally trapped wave has to have one-eighth, five-eighth or nine-eighth, etc., wavelengths between the ground and the turning point. We find that this condition is approximately satisfied by every resonant solution calculated numerically—an indication that the WKB solution is a good approximation for the wind profiles relevant to the real atmosphere.

5. Equilibrium solution in the presence of Ekman pumping

When Ekman damping in the planetary boundary layer is considered, the lower boundary condition [Eq. (3)] should be replaced by (see Part I)

$$\left(\frac{\partial}{\partial t} + \bar{u}\frac{\partial}{\partial x}\right)\Phi'_{z^*} - \frac{S}{gH}\frac{\partial}{\partial x}\Phi' - \bar{u}_{z^*}\frac{\partial}{\partial x}\Phi' + \frac{S}{f_0^2}a_e\nabla^2\Phi' = -\frac{S}{H}w_f,$$

at

$$z^* = z_0^*, \tag{20}$$

where z_0^* denotes the top of the Ekman layer ($z_0^* \sim 1$ km/H) and $w_f = ik\bar{u}\hbar_0[e^{ikx}\sin l(y_p - y)]$ is one Fourier component of the topographically induced vertical velocity at the lower boundary. Above the planetary boundary layer, Eq. (1) continues to hold when dissipation in the interior of the atmosphere is neglected. The solution can still be written as the sum of a stationary forced wave and a travelling wave [cf. Eq. (4)] as

$$\Phi'(x,y,z^*,t) = [e^{ikx}\sin l(y_p - y)]e^{z^*/2} \times \{\phi_{z^*}^{(0)} + \phi_{z^*}^{(1)}\exp[-ikt - \hat{a}_e t]\}, \tag{21}$$

where $\phi^{(0)}$, the stationary forced wave, satisfies Eq. (5) and the boundary condition

$$\phi_{z^*}^{(0)} + (\tfrac{1}{2} - \bar{u}_{z^*}/\bar{u})\phi^{(0)} + \frac{iS(k^2 + l^2)}{f_0^2 k\bar{u}}a_e\phi^{(0)} = -\frac{S\hbar_0}{H}$$

at

$$z^* = z_0^*. \tag{22}$$

The governing equation and boundary condition for the traveling wave, $\phi^{(1)}(z^*)$, can be easily derived by substituting (21) into Eq. (1) and the homogeneous part of Eq. (20). The solution, however, is rather complicated and will not be given here. The temporal behavior of the resonant solution is qualitatively the same as that for the constant $\bar{u}$ case considered in Part I: Initially, when $\hat{a}_e t \ll 1$, the resonant solution amplifies linearly, as given by (19). The linear time growth eventually tapers off to an equilibrium amplitude given by the forced wave only, i.e.,

$$\Phi'(x, y, z^*, t \to \infty) = [e^{ikx}\sin l(y_p - y)]e^{z^*/2}\phi^{(0)}(z^*). \tag{23}$$

For the case where the zonal wind profile is such that the forced wave solution represents an internally trapped wave, the solution (not necessarily resonant) that satisfied the upper boundary condition of boundedness is given by (13). Such a solution has the property that $\Delta(z^*) \equiv \phi_{z^*}^{(0)}(z^*)/\phi^{(0)}(z^*)$ is real.

The magnitude of the wave amplitude at z_0^* is found from Eq. (21) to be

$$|\phi_{z_0^*}^{(0)}| = \frac{S\hbar_0}{H}\left\{[\Delta(z_0^*) + (\tfrac{1}{2} - \bar{u}_{z^*}/\bar{u})_{z_0^*}]^2 + \left[\frac{S^2(k^2 + l^2)^2}{f_0^4 k^2\bar{u}^2}a_e^2\right]\right\}^{-1/2}, \tag{23}$$

from which it can be inferred that the enhanced (resonant) response occurs when the first term in brackets in (23) vanishes, i.e.,

$$\phi_{z^*}^{(0)} + (\tfrac{1}{2} - \bar{u}_{z^*}/\bar{u})\phi^{(0)} \quad \text{at} \quad z^* = z_0^*. \tag{24}$$

Eq. (24) is the same as the resonance condition for the inviscid waves discussed in Sections 3 and 4. The presence of Ekman pumping does not alter the

[5] The heat flux for a resonant wave can be calculated from (19) as

$$\overline{v'T'} = \frac{S^2\hbar_0^2}{H^2F^2f_0R}\frac{1}{2}k^2t\sin^2 l(y_p - y)\left[\frac{\alpha_r^{(0)}(0)}{\alpha_r^{(0)}(z^*)}\right]\left[\frac{\sin p^{(0)}(z^*)}{\sin p^{(0)}(0)}\right]^2 e^{z^*} \times \frac{\partial}{\partial z^*}\left[\cot p^{(0)}(z^*)\int_{z^*}^{z_T^*}q_r(z^*)dz^* - \tfrac{1}{2}q_r(z^*)/\alpha_r^{(0)}(z^*)\right].$$

condition for resonance but it gives a limiting equilibrium amplitude to the resonant solution

$$\phi^{(0)}_{\max}(z^*_0) = \frac{f_0^2}{H}\frac{(ik\bar{u}\hbar_0)}{(k^2+l^2)}\frac{1}{a_e}. \tag{25}$$

This turns out to be exactly the same as the expression for the equilibrium amplitude discussed in Part I for the constant $\bar{u}$ case [cf. Eq. (51), Part I]. Extensive tables for $(\Phi')_{\max}$ have been presented (see Tables 4 and 5 in Part I).[6] The amplitude for the present sheared case is, however, height dependent; Eq. (25) merely gives the amplitude of the density-normalized geopotential height field at the forcing level z^*_0. The vertical structure of the forced wave will be calculated in the next section by numerically solving Eq. (5) subject to the boundedness upper boundary condition. No lower boundary condition will be used; thus one obtains only the ratio $\phi^{(0)}(z^*)/\phi^{(0)}(z^*_0)$. The true amplitude can be calculated by using (25) for the resonant solution, and (23), or equivalently,

$$\phi^{(0)}(z^*_0) = -\frac{S\hbar_0}{H}\left\{[\Delta(z^*_0) + (\tfrac{1}{2} - \bar{u}_{z^*}/\bar{u})_{z^*_0}] + \frac{iS(k^2+l^2)}{f_0^2 k\bar{u}(z^*_0)}\right\}^{-1} \tag{26}$$

when the solution is not at resonance.

6. The finite-difference solution

Having considered the general form of the solutions, we now turn to the explicit solution of the equation using numerical methods. The numerical procedure is very easy if one knows what to look for in the solutions: We will not attempt to determine the time behavior of the solutions, which we have discussed in Sections 4 and 5. We will calculate only the forced wave solution given by (13) and (14), and determine the condition under which the amplitude A becomes infinite.[7]

The equation for the forced wave [Eq. (5)] is written in finite-difference form as (see Lindzen, 1971)

$$y_{m+1} + B_m y_m + y_{m-1} = 0, \quad 1 \leq m \leq M, \tag{27}$$

$$\left.\begin{aligned} B_m &= \lambda^{(0)2}_m(\delta z^*)^2 - 2 \\ \lambda^{(0)}_m &= \lambda^{(0)}(z^*_m), \quad \delta z^* = z^*_{m+1} - z^*_m \\ y_m &= y(z^*_m) \equiv \phi^{(0)}(z^*_m)/\phi^{(0)}(z^*_M) \end{aligned}\right\}. \tag{28}$$

We have normalized $y(z^*_m)$ so that $y_M = 1$. Therefore, the results to be presented give only amplitudes at one height relative to the other. A useful quantity is the ratio $\phi^{(0)}(z^*)/\phi^{(0)}(z^*_0) = y(z^*)/y(z^*_0)$, which can be easily inferred from the graphs to be presented.

The solution is assumed to be evanescent[8] above $z^* = z^*_T$. Therefore the top boundary condition is

$$\frac{d}{dz^*}y(z^*) = -\mu y(z^*) \quad \text{at} \quad z^* = z^*_M, \tag{29}$$

where

$$\mu^2(z^*) = -\lambda^{(0)2}(z^*) \quad \text{for} \quad z^* \geq z^*_T.$$

[In (29), it is assumed that $d\mu/dz^*$ is small at $z^* = z^*_M$.] In centered finite-difference form, (29) is

$$(y_{M+1} - y_{M-1})/2\delta z^* = -\mu_M y_M. \tag{30}$$

We assume, following Lindzen (1971), that the finite-difference solution can be written in the form

$$y_m = \alpha_m y_{m+1} + \beta_m, \tag{31}$$

where α_m and β_m are found by substituting the above form into Eq. (27):

$$\alpha_{m-1} = -1/\alpha_m - B_m, \tag{32}$$

$$\beta_{m-1} = -\beta_m(B_m + \alpha_{m-1}). \tag{33}$$

The upper boundary condition (30) becomes

$$y_M(2 + 2\delta z^*\alpha_M\mu_M + \alpha_M B_M) = 2\beta_M.$$

Since $y_M = 1$ by definition (28), this condition is satisfied by

$$\beta_M = 0,$$

$$\alpha_M = -\frac{2}{B_M + 2\delta z^*\mu_M} = \frac{1}{[1 - \mu_M\delta z^* - \tfrac{1}{2}\lambda^{(0)2}_M\delta z^{*2}]}. \tag{35}$$

Eqs. (34) and (33) together imply

$$\beta_m = 0 \quad \text{for} \quad 1 \leq m \leq M.$$

The α_m's can be calculated using the recursion relation (32) starting with α_M given by (28).

An indication of the resonance is given by y satisfying the homogeneous lower boundary condition [see Eq. (24)]

[6] Note that in these tables the forcing w_f is calculated for $\bar{u} = \beta/(k^2+l^2)$. For $\bar{u}(z^*_0)$ different from this value, a factor $\bar{u}(z^*_0)/[\beta/(k^2+l^2)]$ should be multiplied to the $\Phi'_{\max}$ found from the tables.

[7] As shown in Section 4, the condition that makes A infinite is the same as the resonant condition, and is also the "stationarity" condition, i.e., the condition under which the phase speed of the traveling wave is reduced to zero.

[8] Note that the location of the turning point z^*_T is not preassigned, but is determined internally for each zonal wind profile by the location where $\lambda^{(0)2}(z^*)$ changes sign.

$$\frac{d}{dz^*}y + \left(\frac{1}{2} - \frac{\bar{u}_{z^*}(z^*)}{\bar{u}(z^*)}\right)y = 0 \quad \text{at} \quad z^* = z_0^*, \quad (36)$$

which when translated to centered finite-difference form is the condition

$$\alpha_1 = 2\left\{-B_1 - 2\delta z^*\left[\frac{1}{2} - \frac{\bar{u}_{z^*}(z_0^*)}{\bar{u}(z_0^*)}\right]\right\}^{-1}$$

$$= \left\{1 - \delta z^*\left[\frac{1}{2} - \frac{\bar{u}_{z^*}(z_0^*)}{\bar{u}(z_0^*)}\right] - \frac{1}{2}(\delta z^*)^2\lambda_1^{(0)2}\right\}^{-1}. \quad (37)$$

To test for resonance, we calculate α_m's for a given wind profile and check if the calculated α_1 satisfies Eq. (37).

7. Tests for resonance

In this section we consider various wind profiles constructed within limits that are observationally reasonable and decide what prominent features a resonant profile should possess.

The vertical wind profile that we use in this study is based on the 45°N cross section of a two-dimensional zonal wind field constructed to roughly fit the observed wind conditions. The observed zonal wind field is presented in Fig. 1. Below 30 km the data is taken from Miyakoda (1963) for January 1958, while above 30 km, where the data are sparse, the wind field is constructed based on the climatological field given in CIRA (1972) and requiring that it merge continuously to the wind field of Miyakoda. The prominent features of the climatological wind consist of a stratospheric jet with a jet maximum at around the 60–70 km level; the jet strength is usually around 90 m s^{-1}. The mean wind above 30 km generally increase with height in the stratospheric jet base to the jet maximum. Though a simple calculation (Charney and Drazin, 1961) based on uniform wind speeds shows that 90 m s^{-1} is more than sufficient to trap even the long waves with wavenumbers 1 and 2, the presence of positive shears at the jet base enhances the propagability of the waves considerably [via Eqs. (1) and (2)], so the long waves are usually not trapped until above the jet maximum where the vertical shears start to become negative.

The tropospheric jet is usually located at around the 12–15 km level; its jet strength is about 30 m s^{-1} and seldom exceeds 50 m s^{-1}. In fact below 30 km, the wind field for January 1958 (a sudden warming year) is not too different from other normal years, except possibly for the northward advancement of the zero-wind line.

To fit this wind field and be able to easily change the wind condition functionally, we use the functional form

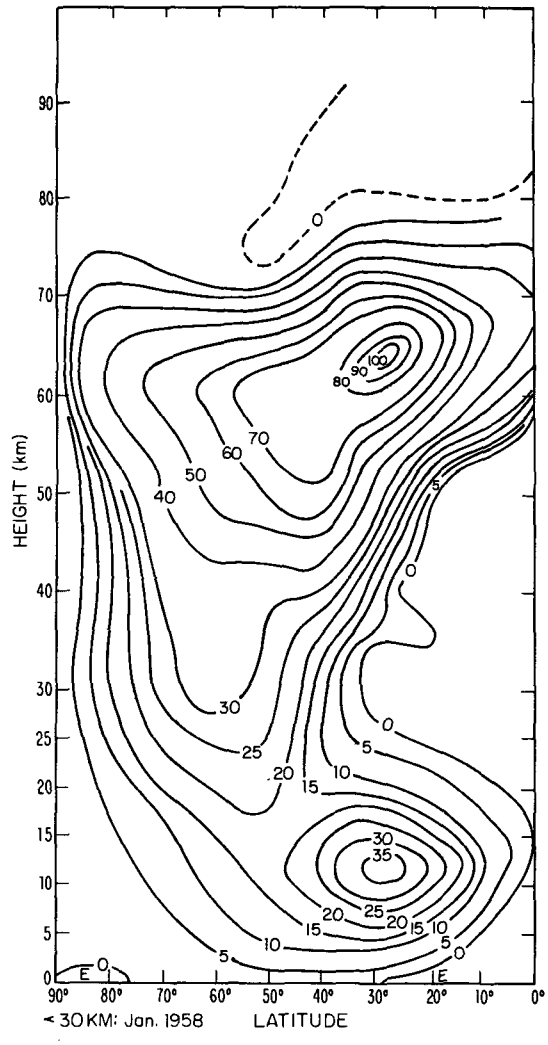

FIG. 1. The "observed" zonal wind field during northern winter. Below 30 km, it is taken from Miyakoda (1963) for January 1958. The wind field above 30 km is constructed based on the climatological field given by CIRA (1972).

$$\bar{u}(\varphi,z^*) = \cos\varphi\{U_0 \tanh[b_0(\varphi - \varphi_0)]$$
$$+ U_1 \operatorname{sech}[b_1(\varphi - \varphi_1)] \operatorname{sech}[a_1(z^* - z_1^*)]$$
$$+ U_2 \operatorname{sech}[b_2(\varphi - \varphi_2)] \operatorname{sech}[a_2(z^* - z_2^*)]\}. \quad (38)$$

In (38), (φ_1,z_1^*) is the location of the tropospheric jet maximum, while (φ_2,z_2^*) is that of the stratospheric jet. φ_0 determines the location of the zero-wind line away from the jet maxima. The strength of the tropospheric jet is given approximately as $\cos\varphi_1\{U_0 \tanh(\varphi_1 - \varphi_0) + U_1\}$, and that of the stratospheric jet as $\cos\varphi_1\{U_0 \tanh(\varphi_2 - \varphi_0) + U_2\}$. The parameters U_0, U_1, U_2, b_0, b_1, a_1, a_2, φ_0, φ_1, φ_2, z_1^* and z_2^* can be chosen to give a best fit to the observed wind field. We sometimes find it necessary to let a_2 take a value for z^* above z_2^* different from the one below. Similarly, a_1 is allowed to have different values above and below z_1^*. There are thus

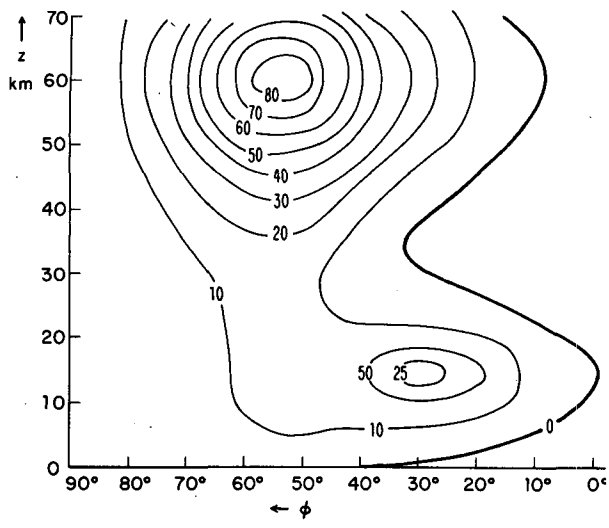

FIG. 2. A typical wind field obtained using the functional formula (38), with $\varphi_0 = 45°$, $\varphi_1 = 30°$, $\varphi_2 = 60°$, $z_1^* = 14$ km/H, $z_2^* = 60$ km/H, $a_1 = 2/12$, $a_2 = 2/20$, $b_0 = 2/10$, $b_1 = 2/30$, $b_2 = 2/30$, $U_0 = 10$ m s^{-1}, $U_1 = 40$ m s^{-1} and $U_2 = 150$ m s^{-1}.

a total of 15 free parameters that we can specify. In Fig. 2 a typical wind field obtained from (38) is presented.

The one-dimensional vertical profiles that are used in this study are calculated using (38) by setting φ at $\pi/4$, i.e., the midlatitude. The full two-dimensional wind field will be used in a later study.

In Fig. 3 one such cross-sectional profile is shown. The jet strengths in this one-dimensional profile are somewhat smaller than the ones in the two-dimensional wind field. This is due to the fact that the latitude we have chosen does not always correspond to the latitudes of the jet maxima. In Fig. 3, the index of refraction squared calculated for this profile is also shown for the modes (s,n) $= (s,1)$ with $s = 1 \ldots 5$. It is seen that the shorter waves $s \geq 4$ are trapped below the tropospheric jet maximum, while the long waves $s = 1$ and 2 are generally not trapped until above the stratospheric jet maximum.

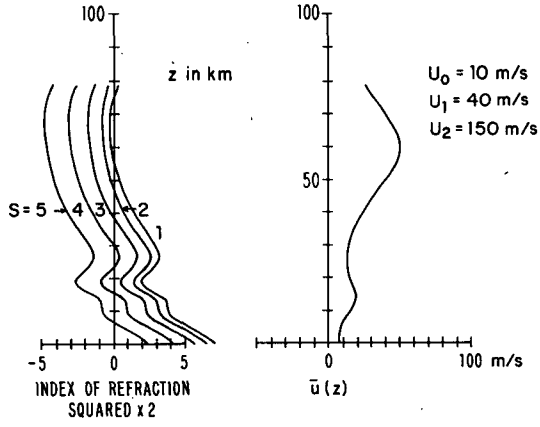

FIG. 3. (Right) Cross-sectional profile of Fig. 2 at the midlatitude. (Left) The square of the index of refraction for the wave modes $(s,n) = (s,1)$, $s = 1, 2, 3, 4$ and 5, corresponding to the profile at right.

The internally trapped wave solutions are shown in Fig. 4. It is seen that for the profile shown in Fig. 3, the mode $(s,n) = (4,1)$ has no node in the vertical, while $(s,n) = (3,1)$ has one and $(s,n) = (2,1)$ has two nodes in the vertical. The mode $(s,n) = (1,1)$ is not trapped and is therefore not shown.

We proceed next to determine the wind configuration that would make a wave mode resonant [i.e., satisfying Eq. (37)]. Wavenumber 4 is considered first. It is clear that the wave mode (4,1), which is internally trapped in the troposphere, should not be affected by changes in wind speeds in the stratosphere, which is above its turning point. Changes in tropospheric jet strength (U_1) affect the solution in the troposphere somewhat, but the corresponding changes in the values of α_1 are so small that it is very difficult to affect the resonance condition (37) by varying U_1 alone. An effective way of altering α_1 is to change the wind speed near the surface as shown in Fig. 5, where a resonant solution is obtained for the mode (s,n) $= (4,1)$ by simply increasing the wind speed below the tropospheric jet slightly.

The effect on the long waves of increasing the stratospheric jet strength is investigated next. The results are shown in Fig. 6 for the mode (2;1). To make the wave resonant,[9] the stratospheric jet strength (U_2) has to increase to more than three times its normal value. Since such abnormal changes have never been observed, we conclude that the increase in stratospheric jet strength is ineffective in making a wave resonant. However, since the trapping of the wave is a prerequisite for resonance, the increase in stratospheric winds that is usually observed preceding a warming event may be important in changing a radiating wave into an internally trapped wave.

In Fig. 7 we show the effects of the descent of the stratospheric jet. By lowering the location of the stratospheric jet maximum (changing z_2^* in our model) from the climatological value of ~60 km, we observe drastic differences in the vertical behavior of the wave solutions. The descent of the jet maximum lowers the turning point of the solution, thus shortening the wave path that a wave has to travel between reflections, and reducing the number of nodes in the vertical structure. α_1 is also significantly changed, presumably due to the change in

[9] It is also possible to make the mode (2,1) resonant by *decreasing* U_2 slightly, but the resulting solution will have two nodes in the vertical. This is not a favorable configuration when damping is present.

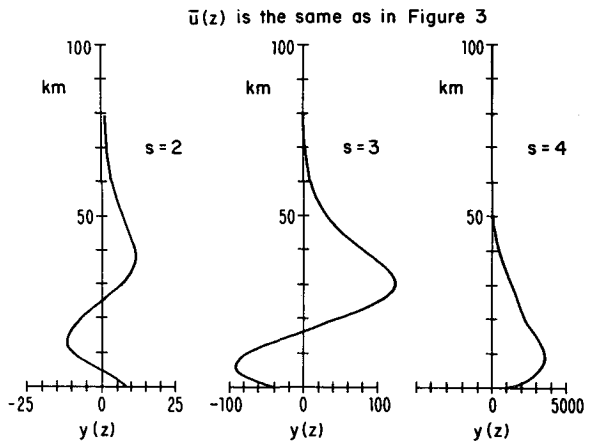

FIG. 4. Internally trapped wave solution $y(z^*)$ for the profile shown in Fig. 3.

phase in the vertical structure by the lowering of the turning point. We find a resonant solution for the mode $(s,n) = (2,1)$ when the jet maximum is lowered to 46 km.

The behavior of the mode $(s,n) = (1,1)$ with respect to changes in jet strength and the lowering of the stratospheric jet is shown in Fig. 8. Since the normal profile shown in Fig. 3 does not trap this wave mode, we increase the stratospheric jet strength until trapping occurs. Continued increase to 65 m s^{-1} at 45°N (i.e., $U_2 = 220$ m s^{-1}, a large but not unreasonable value) gives a resonant solution with two nodes in the vertical. As will be discussed in a later section, because of its short vertical wavelengths and long wave paths, this wave is relatively more susceptible to damping and is not likely to be resonant in the real atmosphere. By lowering the jet maximum to 45 km, another resonant solution is obtained, this time with only one node and a shorter wave path. For a weaker stratospheric jet, the wave mode $(s,n) = (1,1)$ becomes resonant only when the jet is lowered to below 45 km.

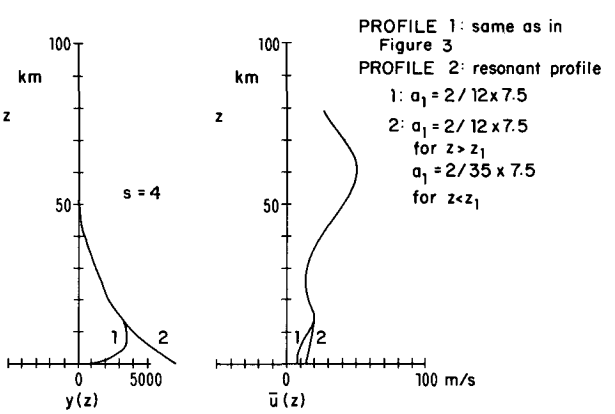

FIG. 5. (Right) Two wind profiles differ slightly only below the tropospheric jet maximum. Profile (2) has an increased lower level wind speed. (Left) Wave $(s,n) = (4,1)$ response to profiles (1) and (2). Solution denoted by (2) is resonant [α_1 satisfying Eq. (37)] and has approximately one-eighth of a wavelength between the turning point and the ground.

Thus it seems that the descent of the stratospheric jet may be a favorable condition for sudden warmings. This is consistent with observations available below 30 km, which show abnormally high wind speeds at the 25–30 km levels preceding the warming events. A recent analysis due to Quiroz *et al.* (1975) does show that on 24 January 1973, just before the onset of a major warming event of wavenumber 1, the stratospheric jet was observed to be located at around 35 km. Though the data used in that study are sparse and more observations are needed to confirm it, the hypothesis of jet descent seems to be consistent with theory as well as present observations and should merit further study.

We have also repeated the calculations for the waves (1,0) and (2,0), which have no nodes in the meridional direction. It was shown in Part I that the mode (1,0) is forced by a rather large component of topographic forcing but the resonant condition for this mode is too stringent. The same conclusion is also reached here in a sheared atmospheric mode; we find the mode (1,0) to be radiating in character and cannot be resonated by physically reasonable wind profiles. The resonance requirement of the mode (2.0), on the other hand, is close to that for the mode (1,1), since the quantity $(k^2 + l^2)$ has values not too different for the two modes. There seems to be the possibility that the two modes can be simultaneously resonated by the same profile.

8. Damping and residence time scales

Unlike the barotropic wave in the uniform wind model considered in Part I, a resonant internal wave in an atmosphere with vertical shears may in principle have many vertical modes. However, we have shown in Section 7 that *under the range of midlatitude profiles realizable in the atmosphere*, the longest planetary waves ($s = 1$ and 2) probably have only two vertical modes, one with two nodes in the vertical structure and the other with one node. It is also shown that the mode with two nodes is easier to excite. That is, it can be excited with a profile that is closer to the "climatological" one, than the mode with only one node in the vertical direction. We have conjectured that the mode with two nodes is more susceptible to damping in the atmosphere and is thus less likely to establish itself as a mode.

To give a measure of a wave's vulnerability to dissipation, we define the "residence time" $t_R(z^*)$ to be

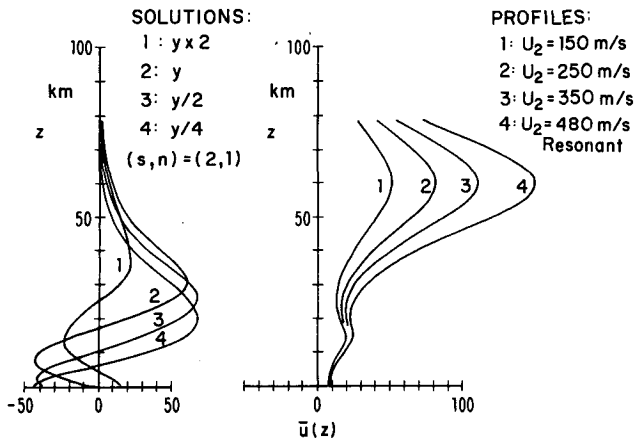

FIG. 6. Wave solutions (left) for $(s,n) = (2,1)$ in response to increases in the stratospheric jet strength (right). Profile (4) is resonant, as its calculated value of α_1 satisfies Eq. (37). The resonant solution has five-eighths of a vertical wavelength between the turning point and the ground.

$$t_R(z^*) = 2\int_0^{z^*} \frac{1}{c_g(z^*)}\,dz^* = \int_0^{z^*} \frac{S}{f_0^2}\,\frac{\hat{\beta}}{k\bar{u}^2}\,\frac{1}{\lambda^{(0)}}\,dz^*,$$

where c_g is the vertical group velocity of the wave. $t_R(z^*)$ gives an estimate of the amount of time a wave spends to traverse a height z^* and back. If the calculated $t_R(z^*)$ for a particular wave mode is of the same order of, or larger than, the time scale of dampings present in the same atmospheric layer, then we say that the wave is very susceptible to damping and it is unlikely to form a resonant mode. On the other hand, if the residence time is found to be considerably smaller than the local damping time scales, the wave is probably less likely to be attenuated by damping and the formation of a resonant mode is then possible.

For the climatological profile in Fig. 3, $t_R(z^*)$, as given above, is evaluated for different zonal wavenumbers and for z^* up to their respective turning points. The result is depicted in Fig. 9. The effects of the lowering of the stratospheric jet maximum on the residence times are shown in Fig. 10 for $s = 1$, and in Fig. 11 for $s = 2$.

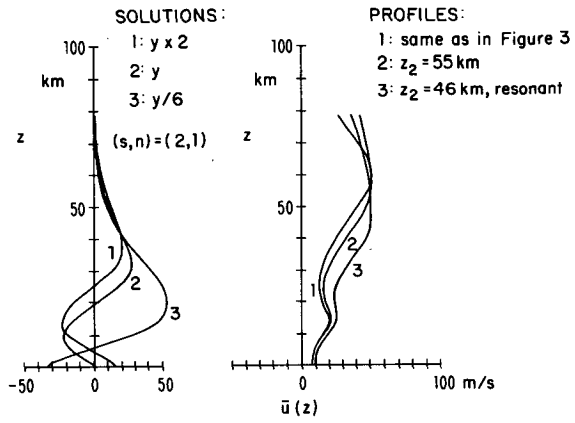

FIG. 7. Wave solutions (left) for $(s,n) = (2,1)$ in response to the descent of the stratospheric jet maximum (right). Profile (3) is the resonant solution when the jet descends to 46 km level.

Fig. 9 shows that, under "normal" circumstances, the time it takes for wavenumber 1 to travel from the surface to its turning point near the 60 km level is rather long (~25 days). This fact tends to suggest that for time scales less than a month, this wave should be considered for practical purposes as a radiating wave. That is, reflections from the upper atmosphere are probably not very significant. Wavenumber 2, on the other hand, completes the round trip from the surface to its turning point near the 50 km level and back in less than four weeks. Therefore reflections from the top should be considered for this wave. However, the reflections are probably diminished considerably by the presence of dampings due to radiative and photochemical processes; the latter is thought to have a rather short damping time scale (of less than a week) in the region around 50 km (Blake and Lindzen, 1973; Dickinson, 1973). Wavenumber 3 is expected to be less susceptible to the photochemical dampings, as its energy is mainly confined to below the 40 km level. Wavenumber 4, being mostly trapped to below the tropopause, is expected to be relatively immune from the effects of radiative and photochemical dampings. Dissipation due to diffusion in the lower atmosphere above the planetary boundary layer is thought to have damping time scales of the order of several weeks.

Fig. 10 shows the effects on the residence time for wavenumber 1 when the number of nodes in the solution is reduced from two in profile (1) to one in profile (3) by the lowering of the jet maximum. The total residence time is cut by about a half. What is more significant is the fact that the mode with one node is confined in a lower portion of the atmosphere and spends less than 3 days in the region above 30 km. We expect this mode to be more realizable in the real atmosphere than the mode with two nodes. The same trend can also be established for wavenumber 2 as depicted in Fig. 11.

9. Summary of results

From the discussions in previous sections concerning the idealized atmospheric model with vertical shears only, the following results have been obtained which may be of relevance to the vertical propagation of atmospheric waves and their resonance. The modification due to the presence of two-dimensional shears will be discussed in a future paper.

1) In the presence of wind profiles, typical of midlatitude vertical distribution of atmospheric wind

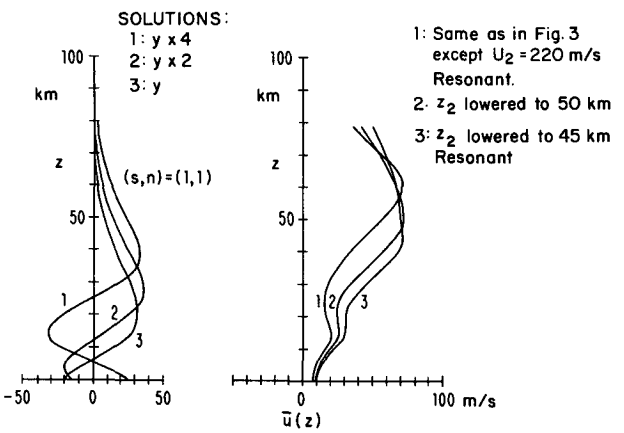

FIG. 8. Wave solutions (left) for $(s,n) = (1,1)$ in response to the descent of the stratospheric jet maximum (right). Profile (1) is the same as in Fig. 3 except with U_2 increased from the climatological value to trap the wave mode. With the jet speed of 65 m s^{-1} at 40°N, profile (1) makes the solution resonant. However, the resonant solution has two nodes. To reduce the number of nodes in the vertical, the location of the jet maximum has to be lowered to the 45 km level [profile (3)]. The solution corresponding to profile (3) is also resonant, with five-eighths of its vertical wavelength between the turning point and the ground.

fields, the shorter stationary planetary waves (with zonal wavenumbers 4 and up) are found to be trapped to below the tropospheric jet maximum. These waves are little affected by changes in wind condition in the stratosphere. The structure of these waves is readily altered and they become resonant when the wind condition in the lower troposphere is varied. The amplifying ridges of these resonant waves may be the cause for the frequent occurrences of shorter scale blocking phenomena in the troposphere.

2) The nature and vertical structures of the longer planetary-scale waves (with zonal wavenumbers 1 and 2) depend crucially on the wind conditions in both the stratosphere and troposphere; therefore they cannot be studied in a tropospheric model that excludes the stratosphere by placing a lid at the tropopause. Large-scale tropospheric blockings are observed to be preceded by significant wind changes in the stratosphere and occur simultaneously with the stratospheric sudden warming phenomenon. In the present theory of resonant Rossby waves, it is hypothesized that both phenomena are caused by the same Rossby wave which becomes resonant with respect to the lower boundary stationary forcings under favorable wind conditions.

3) It is found that wavenumber 1 is usually (climatologically) radiating in character and therefore this wave cannot be resonantly excited under normal wind conditions, as its energy is constantly radiated away to the top of the atmosphere. However, it may become trapped slightly above the stratospheric jet maximum if the jet strength is increased as it is observed to do before the onset of sudden warmings. Wavenumber 2, on the other hand, is normally trapped by the stratospheric jet maximum.

4) In addition to the containment of the wave energy, the waves have to satisfy an additional "stationarity" requirement in order to become resonant with respect to the stationary forcings of topography and heating. The condition is found to be approximately

$$\lambda^{(0)}(0) \tan\left[\int_0^{z_T^*} \lambda^{(0)}(z^*)dz^* + \pi/4\right] + [\tfrac{1}{2} - \bar{u}_{z^*}(0)/\bar{u}(0)] = 0, \quad (39)$$

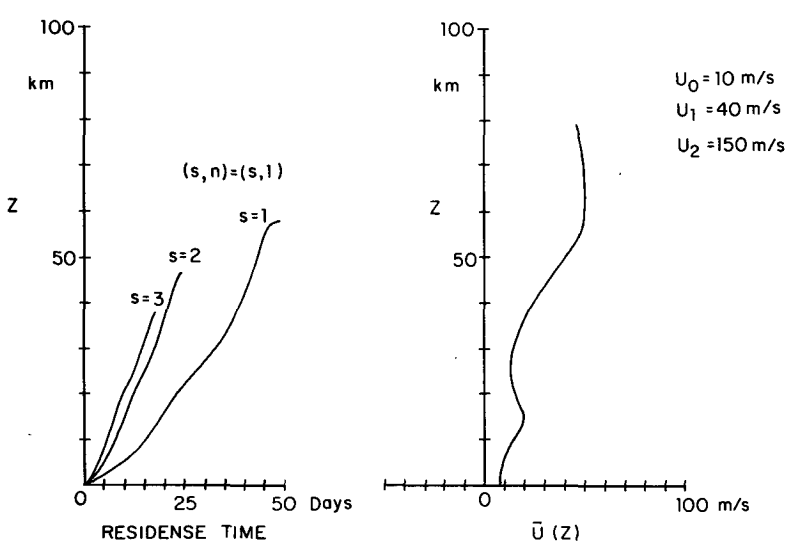

FIG. 9. Residence time $t_R(z^*)$ (left) for $(s,n) = (s,1)$, $s = 1, 2$ and 3 for the climatological profile (right). The profile is the same as that in Fig. 3.

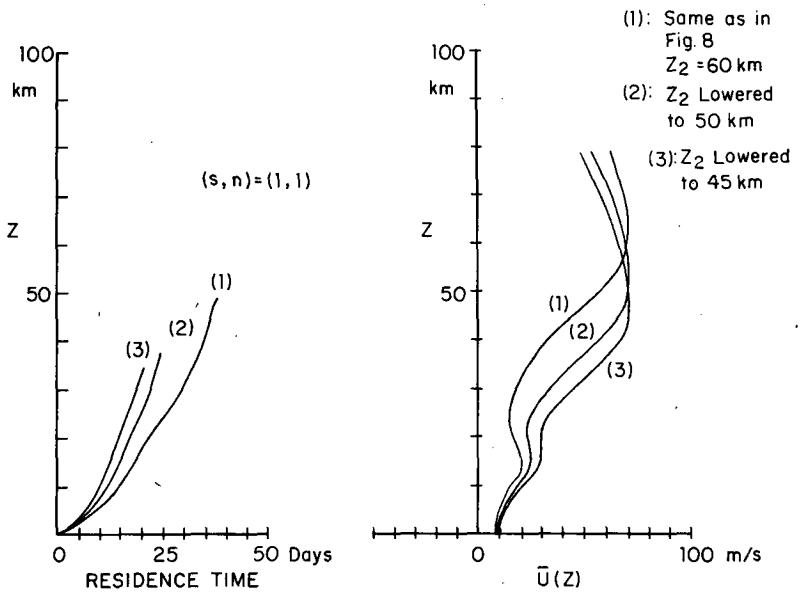

FIG. 10. Residence time $t_R(z^*)$ (left) for $(s,n) = (1,1)$ in response to the lowering of the stratospheric jet (right). The profiles (1), (2) and (3) are the same as those in Fig. 8, which also shows that profile (1) makes the wave mode resonant with two nodes in the vertical while profile (3) reduces the resonant solution to having only one node in the vertical.

where

$$\lambda^{(0)}(z^*) \equiv \left\{ \frac{S}{f_0^2} \left[\frac{\beta - \frac{f_0^2}{S}(\bar{u}_{z^*z^*} - \bar{u}_{z^*})}{\bar{u}(z^*)} - (k^2 + l^2) \right] - \frac{1}{4} \right\}^{1/2}$$

is the "index of refraction" for the vertical propagating wave. Eq. (39) is a condition on the wind profile $\bar{u}(z^*)$ and since both the magnitude and shape of the atmospheric zonal wind enter into the condition, there are, in principle, an infinite number of ways to satisfy the resonance condition. During a season, as the mean wind evolves in time (slowly), the phase speeds of the normal mode planetary waves change also. If the mean wind is such that it satisfies Eq. (39), for a particular wave (k,l), then

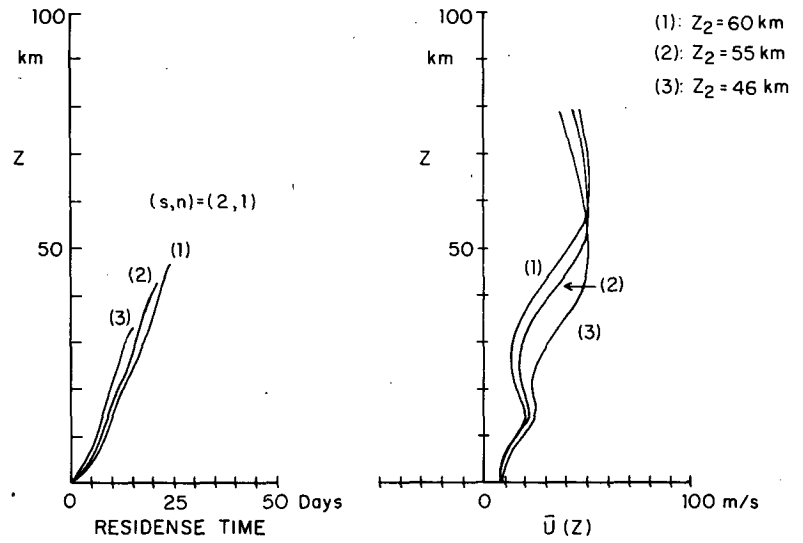

FIG. 11. Residence time $t_R(z^*)$ (left) for $(s,n) = (2,1)$ in response to the lowering of the jet (right). The profiles (1), (2) and (3) are the same as those in Fig. 7, with profile (3) giving a resonant mode with only one node in the vertical.

the phase speed of that wave is reduced to zero and the wave is therefore stationary with respect to the topography. Resonance of that wave mode results and the wave starts to amplify in time.

5) Our numerical experiments suggest that the resonance condition is *not* difficult to meet, as long as the wave's energy is mostly contained. However, most of the resonant modes for the long waves have many nodes in the vertical and therefore the vertical wavelengths are short. These modes presumably are more susceptible to the effects of dissipation which is present in the real atmosphere than the modes with the fewest possible nodes. It is found that under physically reasonable wind conditions, the lowest resonant mode that can be realized for waves with zonal wavenumbers 1 and 2 has one node in the vertical. This mode is excited when the stratospheric jet maximum descends to the vicinity of the 40 km level.

6) Because there still exists considerable uncertainty concerning the magnitude of the forcings at the lower boundary, we have presented our results on wave amplitudes only in normalized form. The reader can calculate the equilibrium amplitude of the wave if the lower boundary forcing is known by using the formula

$$A(z^*) \equiv \frac{1}{g}\frac{\Phi'(x, y, z^*, t \to \infty)}{[e^{ikx}\sin l(y_p - y)]}$$
$$= \frac{1}{g}\phi^{(0)}(z_0^*)\frac{y(z^*)}{y(z_0^*)}\exp[\tfrac{1}{2}(z^* - z_0)],$$

where $\phi^{(0)}(z_0^*)$ is given by (26) when the wave is not at resonance and by (25) at resonance. An important feature of the present solution in the sheared flow is the approximate $e^{z^*/2}$ increase in wave amplitude with height below the turning point. This aspect of the solution is absent in the constant wind model studied in Part I. Waves with zonal wavenumbers 1 and 2, which are not trapped in the troposphere, will have significant influence on the circulation of the stratosphere, especially if these waves are resonant.

Acknowledgment. The authors wish to acknowledge the support of the National Science Foundation through Grant ATM-75-20156 and National Aeronautics and Space Administration through Grant NGL-22-007-228. This paper forms a portion of the Ph.D. thesis of K. K. Tung.

APPENDIX A

List of Symbols

s	zonal wavenumber; number of waves in a zonal circle
f	Coriolis parameter [$=2\Omega\sin\varphi$ where φ is the latitude]
f_0	$2\Omega\sin\varphi_0$, $\varphi_0 = 45°$
β	$\frac{1}{a}\frac{d}{d\varphi}f$ at $\varphi = \varphi_0$, where a is the radius of the earth
S	stability parameter [$=\kappa gH$, where H is the scale height and $\kappa = 2/7$]
h_0	amplitude of a Fourier component of the topographic elevation (plus equivalent elevation due to land-sea differential heating)
k	dimensional zonal wavenumber [$=s/a\cos\varphi$]
l	dimensional meridional wavenumber; its quantization is given in Part I as $l_n = (\frac{1}{2} + n)\pi/(\pi/2)a$, $n = 0, 1, \ldots$
n	number of nodes in the meridional domain
y_p	β-plane's equivalent location of the pole [$=\pi/2a$]
$\lambda^{(0)}$	index of refraction for stationary waves, defined in Eq. (6)
$\lambda^{(1)}$	index of refraction for traveling waves with phase speed c, defined in Eq. (9)
$\alpha^{(0)}$	the variable wavenumber of the standing waves [satisfies Eq. (12)]; its WKB approximation is $\lambda^{(0)}$
$\alpha_r^{(0)}$	the real part of $\alpha^{(0)}$
$\alpha^{(1)}$	same as $\alpha^{(0)}$, except for traveling waves
$\alpha_r^{(1)}$	the real part of $\alpha^{(1)}$
χ	inversely proportional to the amplitude of the forced wave; $\chi = 0$ is the resonance condition
$p^{(0)}(z^*)$	$\int_{z^*}^{z_T^*}\alpha_r^{(0)}dz^* + \pi/4$, where z_T^* is the turning point where $\lambda^{(0)2}$ changes sign
$p^{(1)}(z^*)$	$\int_{z^*}^{z_T^*}\alpha_r^{(1)}dz^* + \pi/4$
μ^2	$-\lambda^{(0)2}$
α_1	first element of α_m defined in Eq. (32); resonance occurs when α_1 satisfies Eq. (37)
U_1	parameter that determines the strength of the tropospheric jet in Eq. (31)
U_2	determines strength of the stratospheric jet in Eq. (38)
z_1^*	vertical location of the tropospheric jet maximum
z_2^*	vertical location of the stratospheric jet maximum
q_r	real part of q [defined in (C7)]
Φ'	perturbation geopotential height
w_0	vertical velocity at the surface

APPENDIX B

Radiating and Trapped Solutions

We are interested in obtaining the general *form* of the solution to Eq. (5), i.e., to

$$\frac{d^2}{dz^{*2}}\phi^{(0)} + \lambda^{(0)2}(z^*)\phi^{(0)} = 0, \tag{B1}$$

subject to a radiating or boundedness upper boundary condition. If

$$\lambda^{(0)2}(z^*) > 0 \quad \text{for} \quad z^* \to \infty,$$

the appropriate solution should be a wave that radiates energy upward to infinity. This condition is satisfied if the solution is written in the form

$$\phi^{(0)}(z^*) = A \exp\left[i \int^{z^*} \alpha^{(0)}(z^*)dz^* \right], \tag{B2}$$

where it is assumed that

$$\text{Re}\ \alpha^{(0)}(z^*) > 0 \quad \text{as} \quad z^* \to \infty.$$

In order that (B2) is a solution of (B1), $\alpha^{(0)}(z^*)$ has to satisfy the Riccati-type equation

$$\alpha^{(0)2} - i\frac{d}{dz^*}\alpha^{(0)} = \lambda^{(0)2}(z^*), \tag{B3}$$

as can be shown by substituting (B2) into (B1).

It is more difficult to obtain the internally trapped solution due to the fact that a pair of propagating wave solutions has to be connected across the turning point z_T^*, where $\lambda^{(0)2}$ changes sign, to an exponentially decaying solution at $z^* \to \infty$. A connection formula is needed. This has been discussed in length in Dingle (1973) and the formula is derived by examining the behaviors of the solutions on crossing the Stoke's lines: Let $\phi_+^{(0)}$ and $\phi_-^{(0)}$ be the exponentially growing and decaying solutions, respectively, at infinity. It can be shown that they have the following forms for $z^* \geq z_T^*$:

$$\phi_+^{(0)}(z^*) = \exp\left[+ \int_{z_T^*}^{z^*} \kappa_+^{(0)}(z^*)dz^* \right], \tag{B4}$$

$$\phi_-^{(0)}(z^*) = \exp\left[- \int_{z_T^*}^{z^*} \kappa_-^{(0)}(z^*)dz^* \right], \tag{B5}$$

where

$$\text{Re}\ \kappa_\pm^{(0)} > 0 \quad \text{for} \quad z^* > z_T^*$$

and satisfy

$$\kappa_+^{(0)2} + \frac{d}{dz^*}\kappa_+^{(0)} = -\lambda^{(0)2}(z^*), \tag{B6}$$

$$\kappa_-^{(0)2} - \frac{d}{dz^*}\kappa_-^{(0)} = -\lambda^{(0)2}(z^*). \tag{B7}$$

For $z^* \leq z_T^*$, we rewrite

$$\kappa_\pm^{(0)} = i\alpha_\pm^{(0)}$$

so that $\text{Re}\alpha_\pm^{(0)} > 0$ for $z^* < z_T^*$, and (B4)–(B7) become

$$\phi_+^{(0)}(z^*) = \exp\left[i \int_{z_T^*}^{z^*} \alpha_+^{(0)}(z^*)dz^* \right], \tag{B8}$$

$$\phi_-^{(0)}(z^*) = \exp\left[-i \int_{z_T^*}^{z^*} \alpha_-^{(0)}(z^*)dz^* \right], \tag{B9}$$

$$\alpha_+^{(0)2} - i\frac{d}{dz^*}\alpha_+^{(0)} = \lambda^{(0)2}(z^*), \tag{B10}$$

$$\alpha_-^{(0)2} + i\frac{d}{dz^*}\alpha^{(0)} = \lambda_-^{(0)2}(z^*), \tag{B11}$$

for $z^* < z_T^*$. The connection formula tells us that the exponentially decaying solution (B5) above the turning point is connected to a pair of up and down going waves (B8) and (B9) below the turning point with a 90° phase shift, i.e., the solution below the turning point can be written as

$$\begin{aligned}\phi^{(0)}(z^*) &= \text{constant} \times [\phi_-^{(0)} + i\phi_+^{(0)}] \\ &= \frac{A}{[\alpha_r^{(0)}(z^*))]^{1/2}} \\ &\quad \times \sin\left[\int_{z^*}^{z_T^*} \alpha_r^{(0)}(z^*)dz^* + \pi/4 \right],\end{aligned} \tag{B12}$$

where $\alpha_r^{(0)}$ is the real part of $\alpha_+^{(0)}$ satisfying (B10). In arriving at the last step in (B12), use has been made of the fact that $\alpha_+^{(0)}$ and $\alpha_-^{(0)}$ are complex conjugates of each other, as can be deduced from Eqs. (B10) and (B11).

APPENDIX C

The Resonant Limit

The forced stationary wave solution is [Eq. (13)]

$$\phi^{(0)}(z^*) = A[\alpha_r^{(0)}(z^*)]^{-1/2} \sin p^{(0)}(z^*), \tag{C1}$$

while the traveling part of the solution is

$$\begin{aligned}&\phi^{(1)}(z^*)e^{-ikct} \\ &\quad = -A[\alpha_r^{(1)}(z^*)]^{-1/2} \sin p^{(1)}(z^*)e^{-ikct},\end{aligned} \tag{C2}$$

and $\alpha^{(0)}(z^*)$ satisfies

$$\alpha^{(0)2} - i\frac{d}{dz^*}\alpha^{(0)} = \lambda^{(0)2}(z^*), \tag{C3}$$

$$\lambda^{(0)2}(z^*) \equiv \frac{S}{f_0^2}\left[\frac{\hat{\beta}(z^*)}{\bar{u}(z^*)} - (k^2 + l^2) \right] - \frac{1}{4},$$

and $\alpha^{(1)}(z^*)$ satisfies

$$\alpha^{(1)2} - i\frac{d}{dz^*}\alpha^{(1)} = \lambda^{(1)2}(z^*), \tag{C4}$$

$$\lambda^{(1)2}(z^*) \equiv \frac{S}{f_0^2}\left[\frac{\hat{\beta}(z^*)}{\bar{u}(z^*) - c} - (k^2 + l^2) \right] - \frac{1}{4}.$$

Since

$$\lambda^{(1)2} \to \lambda^{(0)2} + \frac{S}{f_0^2}\frac{\hat{\beta}}{\bar{u}}\frac{c}{\bar{u}} \quad \text{as} \quad c \to 0,$$

$\alpha^{(1)}$ can be assumed to be

$$\alpha^{(1)} = \alpha^{(0)} + \delta\alpha^{(1)}, \tag{C5}$$

where

$$\delta\alpha^{(1)} = O(c).$$

We write

$$\delta\alpha^{(1)}(z^*) = q(z^*)c. \tag{C6}$$

Substituting (B5) into (B4) shows that $q(z^*)$ satisfies

$$2\alpha^{(0)}(z^*)q(z^*) - i\frac{d}{dz^*}q(z^*) = \frac{S}{f_0^2}\frac{\hat{\beta}(z^*)}{\bar{u}(z^*)^2}. \tag{C7}$$

[Note that $q(z^*)$ is independent of c and is of order 1.] Thus as $c \to 0$, one has

$$[\alpha_r^{(1)}(z^*)]^{-1/2} \to [\alpha_r^{(0)}(z^*)]^{-1/2}\left[1 - \frac{\frac{1}{2}q_r(z^*)}{\alpha_r^{(0)}(z^*)}c\right],$$

$$\sin p^{(1)}(z^*) = \sin\left[p^{(0)}(z^*) + c\int_{z^*}^{z_T^*} q_r(z^*)dz^*\right] \to \sin p^{(0)}(z^*) + c\int_{z^*}^{z_T^*} q_r(z^*)dz^*\cos p^{(0)}(z^*).$$

The total solution, the sum of (C1) and (C2), becomes

$$\phi^{(0)} + \phi^{(1)}e^{-ikct} = A[\alpha_r^{(0)}(z^*)]^{-1/2}\left\{\sin p^{(0)}(z^*) - [1 - ikct + \cdots]\right.$$
$$\left.\times\left[1 - \frac{\frac{1}{2}q_r(z^*)}{\alpha_r^{(0)}(z^*)}c + \cdots\right]\left[\sin p^{(0)}(z^*) + c\int_{z^*}^{z_T^*} q_r(z^*)dz^*\cdot\cos p^{(0)}(z^*) + \cdots\right]\right\}$$
$$\to Ac\frac{\sin p^{(0)}(z^*)}{[\alpha_r^{(0)}(z^*)]^{1/2}}\left\{ikt - \cot p^{(0)}(z)\int_{z^*}^{z_T^*} q_r(z^*)dz^* + \frac{1}{2}\frac{q_r(z^*)}{\alpha_r^{(0)}(z^*)}\right\}. \tag{C8}$$

The amplitude A has been found in (16) to be

$$A = -\frac{S\hbar_0[\alpha^{(0)}(0)]^{1/2}}{H\sin p^{(0)}(0)}\chi^{-1}, \tag{C9}$$

where

$$\chi \equiv -\alpha_r^{(0)}(0)\cot p^{(0)}(0) + \left[\left(\frac{1}{2} - \frac{\bar{u}_{z^*}(0)}{\bar{u}(0)}\right) - \frac{\frac{1}{2}\frac{d}{dz^*}\alpha_r^{(0)}(0)}{\alpha_r^{(0)}(0)}\right] \tag{C10}$$

and goes to zero at resonance.

To find c, the lower boundary condition Eq. (10) is used, giving

$$-\alpha_r^{(1)}(0)\cos p^{(1)}(0) + \left[\frac{1}{2} - \frac{\bar{u}_{z^*}(0)}{\bar{u}(0) - c} + \frac{c}{\bar{u}(0) - c}\frac{S}{gH} - \frac{1}{2}\frac{d}{dz^*}\alpha_r^{(1)}(0)/\alpha_r^{(1)}(0)\right]\sin p^{(1)}(0) = 0. \tag{C11}$$

The asymptotic relation between c and $\alpha^{(0)}$ is found from (C11) as

$$c = -\chi/F, \tag{C12}$$

where

$$F \equiv \left\{\left[\frac{1}{2} - \frac{\bar{u}_{z^*}(0)}{\bar{u}(0)} - \frac{1}{2}\frac{d}{dz^*}\alpha_r^{(0)}(0)/\alpha_r^{(0)}(0)\right]\cot p^{(0)}(0)\int_0^{z_T^*} q_r dz^* - \left[\cot p^{(0)}(0)q_r(0) - \alpha_r^{(0)}\int_0^{z_T^*} q_r dz^*\right]\right.$$
$$\left. + \left[-\frac{\bar{u}_{z^*}(0)}{\bar{u}(0)^2} + \frac{S}{gH\bar{u}(0)} - \frac{\frac{1}{2}\frac{d}{dz^*}q_r(0)}{\alpha_r^{(0)}(0)} + \frac{\frac{1}{2}\frac{d}{dz^*}\alpha_r^{(0)}(0)}{\alpha_r^{(0)}(0)^2}q_r(0)\right]\right\}. \tag{C13}$$

Therefore, at resonance we have

$$Ac \to \frac{S\hbar_0[\alpha_r^{(0)}(0)]^{1/2}}{H\sin p^{(0)}(0)}F^{-1},$$

so that (C8) is

$$\phi^{(0)}(z^*) + \phi^{(1)}(z^*)e^{-ikct} \to \frac{S\hbar_0[\alpha_r^{(0)}(0)]^{1/2}}{H\sin p^{(0)}(0)\cdot F}\left\{\left[ikt - \cot p^{(0)}(z^*)\int_{z^*}^{z_T^*} q_r(z^*)dz + \frac{\frac{1}{2}q_r(z^*)}{\alpha_r^{(0)}(z^*)}\right]\frac{\sin p^{(0)}(z^*)}{[\alpha_r^{(0)}(z^*)]^{1/2}}\right\}. \tag{C14}$$

REFERENCES

Blake, D., and R. S. Lindzen, 1973: Effect of photochemical models on calculated equilibria and cooling rates in the stratosphere. *Mon. Wea. Rev.*, **101**, 783–802.

Charney, J. G., and P. G. Drazin, 1961: Propagation of planetary scale disturbances from the lower into the upper atmosphere. *J. Geophys. Res.*, **66**, 83–109.

CIRA, 1972: *Cospar International Reference Atmosphere*. Akademik-Verlag, 450 pp.

Dickinson, R. E., 1973: Method of parameterization for infrared cooling between altidues of 30 and 70 kilometers. *J. Geophys. Res.*, **78**, 4451–4457.

Dingle, R. B., 1973: *Asymptotic Expansions: Their Derivations and Interpretation*. Academic Press, 521 pp.

Lindzen, R. S., 1971: Atmospheric tides. *Mathematical Problems in the Geophysical Sciences, Lectures in Applied Mathematics*, Vol. 14, Amer. Math. Soc., 293–360.

Miyakoda, K., 1963: Some characteristic features of winter circulation in the troposphere and lower stratosphere. Tech. Rep. No. 14, Dept. Geophys. Sci., The University of Chicago, 176 pp.

Quiroz, R. S., A. J. Miller and R. M. Nagatani, 1975: A comparison of observed and simulated properties of sudden stratospheric warmings. *J. Atmos. Sci.*, **32**, 1723–1736.